Reversible Collapse of Insoluble Monolayers: New Insights on the Influence of the Anisotropic Line Tension of the Domain

ARTICLE *in* THE JOURNAL OF PHYSICAL CHEMISTRY B · OCTOBER 2009

Impact Factor: 3.3 · DOI: 10.1021/jp9055158 · Source: PubMed

6 AUTHORS, INCLUDING:

Pérez-Morales Marta
University of Cordoba (Spain)
30 PUBLICATIONS **270** CITATIONS
SEE PROFILE

Juan Giner-Casares
CIC biomaGUNE
46 PUBLICATIONS **283** CITATIONS
SEE PROFILE

Luis Camacho
University of Cordoba (Spain)
150 PUBLICATIONS **1,565** CITATIONS
SEE PROFILE

Reversible Collapse of Insoluble Monolayers: New Insights on the Influence of the Anisotropic Line Tension of the Domain

Antonio M. González-Delgado, Marta Pérez-Morales, Juan J. Giner-Casares, Eulogia Muñoz, María T. Martín-Romero, and Luis Camacho*

Departamento de Química Física y Termodinámica Aplicada, Universidad de Córdoba, Campus de Rabanales, Ed. Marie Curie, Córdoba, Spain E-14071

Received: June 12, 2009; Revised Manuscript Received: July 28, 2009

In this paper, we study the collapse of a mixed insoluble monolayer formed by a cationic matrix, dioctadecyl-dimethylammonium bromide (DOMA), and a tetra-anionic porphyrin, tetrakis(4-sulfonatophenyl)porphyrin (TSPP), in a molar ratio TSPP/DOMA = 1:4. During the collapse of this system, we visualized the formation of circular domains consisting exclusively of trilayer, although the domains coalescence was not observed. The coexistence of trilayer and monolayer at the final step of the collapse cannot be interpreted exclusively in terms of a thermodynamic phase equilibrium, intervening as an additional factor the anisotropic line tension of the domain. A high line tension implies a high resistance to the domain deformation, and the anisotropy of the line tension implies the lack of coalescence between these domains, which has been experimentally observed by Brewster angle microscopy for us. Under these circumstances, the domains of collapsed material could enclose monolayer regions where the local surface pressure drops thus stopping the collapse process. The collapse of the TSPP/DOMA system is reversible, that is, the return of the three-dimensional material to the monolayer fits into a simple kinetics according to the nucleation−growth-collision theory. As for the collapse, the reverse process is also affected by the line tension of the domains. This paper relates the high line tension and the anisotropic line tension of a given domains with the reversible nature of the collapse process.

1. Introduction

Monolayer collapse is of capital importance from a nanotechnological point of view, as it is a physical process in which molecules are self-assembled into supramolecular, three-dimensional (3D) structures.[1] Furthermore, monolayer collapse plays a fundamental role in a biophysical system, such as in the pulmonary surfactants.[2] A rationale comprehension of the monolayer collapse, as well as a quantitative model, is highly desirable. A Langmuir monolayer can show two- to three-dimensional phase transitions under overcompression, where modified structures are formed in the direction perpendicular to the water surface. Such a transition occurs at a particular surface pressure called the collapse pressure, and the newly formed state is called the collapse state.[3] In the absence of other phenomena, e.g., soluble aggregates, desorption or evaporation, the monolayer insoluble collapse could be described quantitatively through the decrease in the surface area at constant surface pressure.[4,5]

Although a few systems have been described that seem to collapse toward a bilayer,[6−9] for classical amphiphilic molecules the first step in the collapse is the trilayer formation, but the process could progress toward the multilayer formation. However, some experimental systems have been described where the collapses seem to stop at the trilayer.[10−18] The understanding of the collapse mechanisms for these simple systems is essential to control their possible applications for creating supramolecular architectures by means of the Langmuir−Blodgett technique.

Two different mechanisms have been proposed by which a trilayer can grow from the monolayer of insoluble molecules: (I) the folding of the monolayer, and (II) the direct trilayer growth at the domain edge.[12,13,17,19] In the first case, the bilayer must flow (sliding) over the monolayer. In the second one the domain could be formed both by the bilayer, as the previous case, or by the trilayer, which adopts a more rigid structure than the monolayer.

As demonstrated previously, the mixed monolayers formed by dioctadecyl-dimethylammonium bromide (DOMA) and tetrakis(4-sulfonatophenyl)porphyrin (TSPP) in a molar ratio 4:1, experiment a collapse at high surface pressure.[14] Thus, when an area of $A \approx 0.75$ nm^2/DOMA molecule is reached upon compression and keeping the surface pressure constant ($\pi_c \geq 33$ mN/m), several small circular bright domains can be observed by Brewster angle microscopy (BAM). Those bright domains grow spontaneously filling almost all of the field of view in a few minutes. During this phenomenon, the film area decreases from $A \approx 0.75$ nm^2 at $t = 0$ s to ~ 0.3 nm^2 at $t \rightarrow \infty$. The experimental results obtained confirm that the collapse corresponds to a phase transition between a monolayer and a trilayer with well-defined structure.[14] Also, from ellipsometry measurement we have demonstrated that the bright domains correspond to the trilayer structure.[14] Moreover, the collapse is reversible, that is, when the surface pressure decreases below its collapse value the monolayer is regenerated from the trilayer.

However, in the final step of the collapse process ($A \approx 0.3$ nm^2), the interface is not completely covered by the trilayer, as one would expect for a classical phase transition. We observed that this phenomenon is due to the absence of coalescence between domains which originates monolayer enclosed regions where the local surface pressure drops below the collapse surface pressure. We studied this phenomenon and its influence on the

* To whom correspondence should be addressed. Phone: +34 957 21 86 17. Fax: +34 957 21 86 18. E-mail: lcamacho@uco.es.

10.1021/jp9055158 CCC: $40.75
Published on Web 09/15/2009

experimental $A-t$ relaxation curves is analyzed for the collapse and the reverse process, as well.

2. Experimental Section

Materials. Dioctadecyldimethylammonium bromide was purchased from Sigma Chemical Co. and used as received. Tetrakis (4-sulfonatophenyl) porphyrin was supplied by Fluka and used without purification. A mixture of dichloromethane, methanol, and water with a ratio of 15:9:2 (v/v/v) was used as spreading solvent for solving both components. The pure solvents were obtained without further purification from Panreac (Spain) and Baker Chemicals (Germany). The water for the subphase and for the mixture spreading solvent was prepared with a Millipore Mill-Q unit, pretreated by a Millipore Reverse Osmosis system (>18 MΩ × cm^{-1}).

Preparation of the Mixed Monolayers at the Air−Water Interface. Mixed monolayers of TSPP/DOMA in a molar ratio of 1:4 were prepared by cospreading (the mixed solution of the two components) onto a pure water subphase at 21 °C on a Nima Langmuir trough provided with a Wilhelmy type dynamometric system using a plate of filter paper for good wettability. After cospreading of the mixed solution on the water surface, 15 min were left for evaporation of the solvent and the monolayers were compressed at a speed of ∼0.1 nm^2 min^{-1} $molecule^{-1}$.

Brewster Angle Microscopy. Images via Brewster angle microscopy were obtained with a I-Elli2000 apparatus (supplied by Nanofilm Technologies, Göttingen, Germany) using a Nd:YAG diode laser, which can be recorded with a lateral resolution of 2 μm. The image processing procedure included a geometrical correction of the image, as well as a filtering operation to reduce interference fringes and noise. Furthermore, the brightness of each image was scaled to improve contrast. The microscope and the film balance were located on a table with vibration isolation (antivibration system MOD-2 S, Halcyonics, Göttingen, Germany) in a large class 100 clean room.

3. Results and Discussion

3.1. Area-Time Curves at Constant Collapse Surface Pressure. Monolayers of TSPP/DOMA in a molar ratio of 1:4 were formed at the air−water interface as was described previously.[14] Figure 1 (inset) shows a cyclic $\pi-A$ isotherm where the area, A, is expressed per DOMA molecule. The most noticeable phenomenon observed is the monolayer collapse as the mixed film is compressed at $A < 0.75$ nm^2.

The kinetics of the monolayer collapse has been studied by applying a constant surface pressure. First, the film was compressed to a fixed surface pressure ($\pi_0 = 32$ mN/m) below the collapse surface pressure. After compression, time for stabilization of the film was allowed. A complete stabilization of the film was considered when the molecular area did not change with time. After stabilization, the surface pressure was increased to a new constant value ($\pi_c \geq 33.5$ mN/m). A spontaneous area reduction of the monolayer was registered ($A-t$ curves). Figure 1 shows the area variation as A/A_0 versus time (solid lines), where A_0 is the surface area when π_c is reached ($t = 0$ s) and A is the surface area at a given time t. Four different values of collapse pressure (π_c) have been used, ranging from 33.5−36 mN/m. For the collapse process, the initial area is the maximum area $A_{Max} = A_0$ (0.75 nm^2/DOMA molecule).

As can be seen, the relaxation process occurs in a shorter time as π_c increases. For any value of $\pi_c \leq 36$ mN/m at an infinite time, $A/A_0 \approx 0.4$. For $\pi_c > 38$ mN/m the spontaneous monolayer area reduction occurs in very few seconds, so the collapse starts during the initial compression process ($\pi_0 \rightarrow \pi_c$).

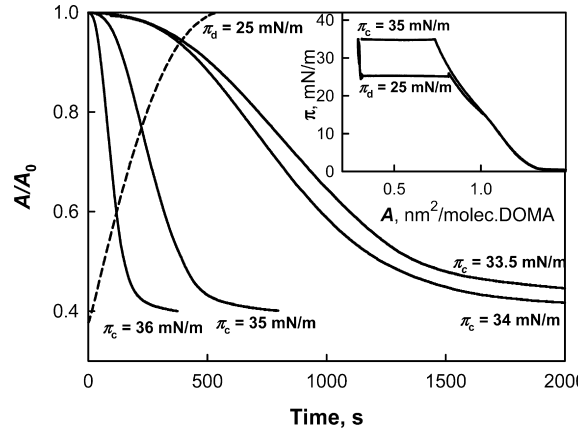

Figure 1. Black solid line: time−area curves (A/A_0 vs t, where $A_0 = A_{Max}$) for four different π_c values, ranges from 33.5−36 mN/m. Black dashed line: area-time curve (A/A_∞ vs t, where $A_\infty = A_{Max}$) for $\pi_d = 25$ mN/m. Inset: Cyclic surface pressure−area isotherms of TSPP/DOMA = 1:4 (solid line) at the air−water interface under compression from 0 to 35 mN/m, evolution with time at $\pi_c = 35$ mN/m, decompression to 25 mN/m, evolution with time at $\pi_d = 25$ mN/m, and decompression from 25 to 0 mN/m.

The A/A_0-t curves show an interesting behavior. Measuring the time (τ) for which a fixed A/A_0 value is reached for the different π_c values, for example for $A/A_0 = 0.8$, the following values are obtained, $\tau = 706$, 632, 206, and 75 s for $\pi_c = 33.5$, 34, 35, and 36 mN/m, respectively. The plot A/A_0 versus t/τ shows that all the curves are superimposed, which is indicative that the collapse mechanism is conserved independently from the applied π_c.

To investigate the stability of the monolayers formed at the air−water interface, successive compression−expansion cycles of the films were carried out. In all the cases small or null hysteresis was observed (see Supporting Information).

3.2. Direct Visualization of Film Morphology by BAM. BAM offers the possibility of visualizing the film morphology directly. Mixed TSPP/DOMA = 1:4 monolayer at the air−water interface was studied by BAM (Figure 2). Monolayer (2D) to trilayer (3D) transformation was observed, as reported for supersaturated monolayers.[20] BAM images were recorded simultaneously in the A versus t measurement. At the initial time ($t = 0$) under a constant surface pressure π_c, the monolayer appears as an homogeneous film (images not shown). After a short time, small bright domains with circular forms appear on the film. The bright domains are surrounded by a darker area. The domains grow spontaneously along their radial direction. For a constant A/A_0 value, the number of domains increases, and the average size of the domain decreases when the applied π_c increases. In any case, for $\pi_c \leq 38$ mN/m at infinite time, the bright domains fill an area fraction of the observed surface of ∼0.8−0.85, while the dark regions fill an area fraction of the observed surface of ∼0.2−0.15, approximately.

During the decompression process the domains disappear completely, as is described below. If a second compression of the film is realized for the same collapse surface pressure, the BAM images show domains with similar form and size that those observed for the first compression step (see Supporting Information), indicating the reversible character of the collapse.

3.3. Failure in the Application of the Classical Nucleation-Growth-Collision (NGC) Theory. The decreasing of the area, A/A_0, versus time, t, as displayed in Figure 1, is a consequence

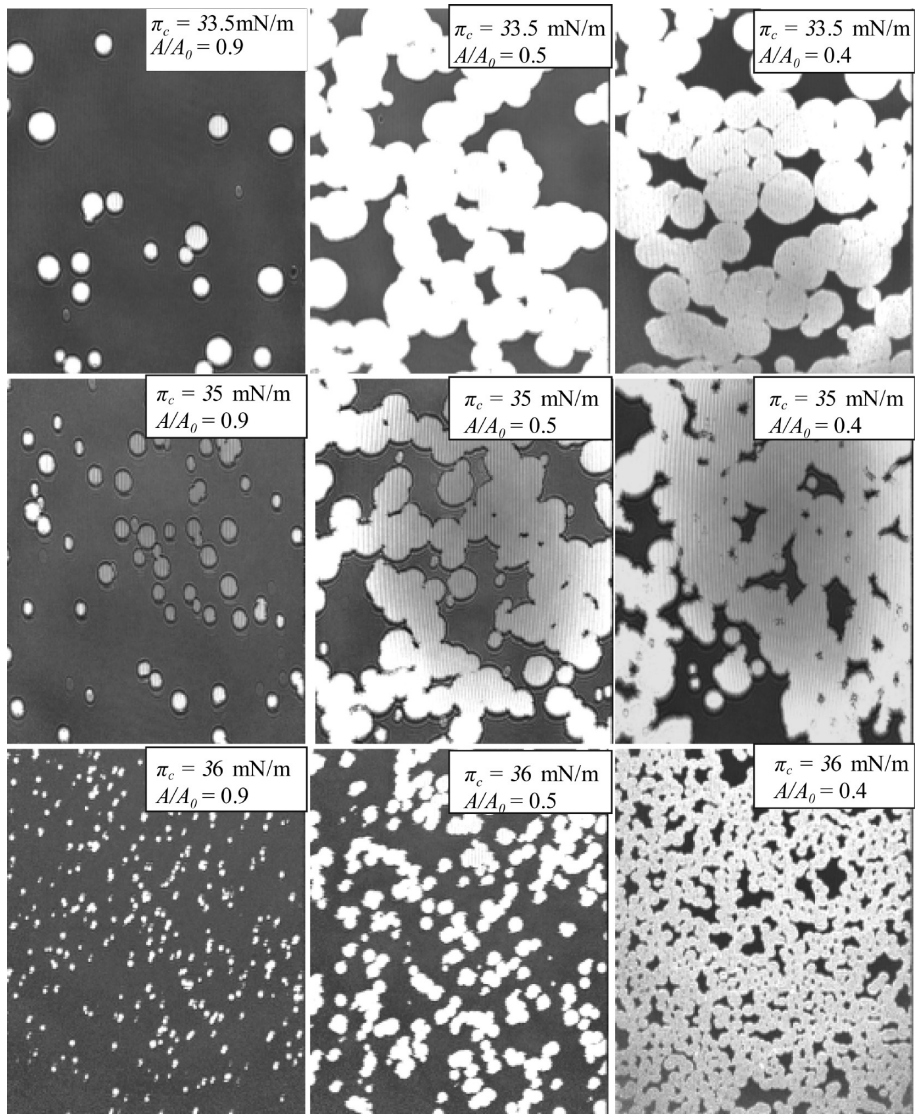

Figure 2. The growing of the domains observed by BAM for π_c = 33.5, 35, and 36 mN/m, at three A/A_0 values for the mixed TSPP/DOMA monolayer. Image size: 400 μm width.

of the transference of monolayer material from monolayer (2D) to trilayer (3D). This behavior could be analyzed by means of the classical NGC theory. This theory was introduced for insoluble monolayers by Vollhardt and Retter.[5,21−23] The NGC theory assumes the formation and subsequent growth of 3D centers, considering the overlap of the growing nuclei in the subsequent stages of the process. According to the model, the variation of area with time is expressed as

$$\frac{A(t)}{A_0} = \frac{A_\infty}{A_0} + \frac{(A_0 - A_\infty)}{A_0} \exp[-k(t - t_{ind})^n] \qquad (1)$$

where A_0 and A_∞ denote molecular area values at initial and infinite time, respectively, k is a constant, t_{ind} is an induction time, and n an integer or semi-integer number, which depends on the nucleation mechanism.

Although it is possible to obtain a good fit between eq 1 and our experimental data, these numerical fits should be interpreted with caution, as shown below. Thus, the experimental data (A/A_0 versus t) were fitted to eq 1 by using $A_\infty/A_0 = 0.4$, and t_{ind}, k, and n as unknown parameters. Figure 3A shows the experimental data for $\pi_c = 35$ mN/m (gray dotted line) and the predictions of eq 1 (solid line). The obtained values for the parameters were $t_{ind} = -13$ s, $k = 0.015$ s^{-n} and $n = 2.51$. As can be seen, there is a general good agreement between experimental data and theoretical predictions. The negative induction time could be related with the elapsed time from the stabilization pressure ($\pi_0 = 32$ mN/m), to the surface pressure π_c. The value $n \approx 2.5$ was obtained for all the π_c values analyzed. This n value corresponds to hemisphere clusters and progressive nucleation.[5]

However, there are two facts that make us think that the good agreement between experimental data and theoretical predictions is circumstantial. First, the nuclei observed in BAM images are cylinders that grow along their edges. Therefore, values of $n = 2$ (instantaneous) or $n = 3$ (progressive) are expected.[5] Second, the NGC theory is based on the collision and overlapping of the growing domain, that is, the NGC theory assumes that in the final step of the monolayer collapse, the whole surface is covered by the 3D domains. In this context, the Avrami expression for the overlapping of growing centers is used to obtain the eq 1.[5,24−26] However, as displayed in Figure 2, in the final step of the monolayer collapse there are regions covered by domains, but there are also regions where the collapse does not take place and the monolayer still persists.

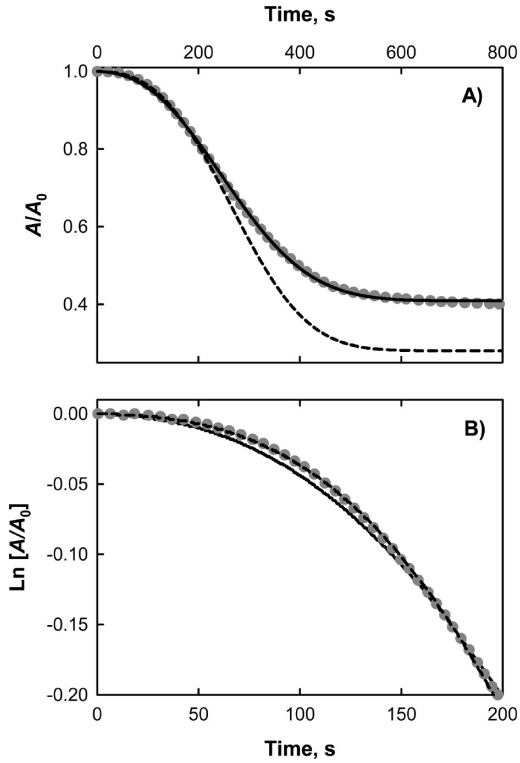

Figure 3. (A) Gray dotted line: experimental A/A_0 vs t data for $\pi_c = 35$ mN/m. Solid line: predictions of eq 1 for $A_\infty/A_0 = 0.4$, $t_{ind} = -13$ s, $k = 0.015$ s^{-n} and $n = 2.51$. Dashed line: predictions of eq 1 for $A_\infty/A_0 = 0.28$, $t_{ind} = -12$ s, $k = 7.296 \times 10^{-3}$ s^{-n} and $n = 2.94$. (B) Plot of $\ln(A/A_0)$ vs t for the same conditions as that of (A).

In Figure 3B plot of $\ln(A/A_0)$ vs t for the experimental data ($\pi_c = 35$ mN/m, gray dotted line), as well for the predictions of eq 1 (solid line, for $t_{ind} = -13$ s, $k = 0.015$ s^{-n} and $n = 2.51$) are shown. The plot is zoomed into the region of the initial times. As can be seen, for these time values there is a slight deviation between the experimental data and theoretical predictions.

An eye on the circular domains formed by $\pi_c = 33.5$ mN/m and $A/A_0 = 0.4$ (see Figure 2), which correspond to an infinity time relaxation, permits us to observe that the domains are in collision, but they neither coalesce nor are deformed. This behavior must be related with the rigid structure of the domains.

3.4. Excluded Surface Regions: Monolayer Existence beyond the Collapse. The BAM images shown by $A/A_0 = 0.4$ in Figure 2 represents the final step of the collapse. Surprisingly, for a $\pi_c \geq 33.5$ mN/m there are regions in which the monolayer persists in the final step of the collapse. Neither the growth of the nuclei nor the appearances of new nuclei are observed hereafter. However, the surface pressure remains constant. From a thermodynamic point of view, new nuclei should be formed in the monolayer regions and the nuclei should continue to grow.

The proposed explanation for this phenomenon is that in regions where the monolayer persists, ("excluded surface" regions for the collapse), the local surface pressure drops below a certain threshold value. This drop in the local surface pressure inhibits the nucleation and the nuclei growth processes. It should be highlighted that this concept implies the existence of regions inside the monolayer under a local surface pressure below collapse surface pressure $\pi < \pi_c$, for a macroscopic situation of a monolayer under a global $\pi > \pi_c$. The origin of these excluded surface regions is explained as follows. When the available area decreases to values close to the collapse final area, some monolayer regions are enclosed by domain collision: excluded surface regions (see black regions in Figure 2 for $A/A_0 = 0.4$, and Scheme 1). The excluded surface regions are isolated from each other. In this way, the collision between collapsed domains might form an interconnected rigid network which sustains extra pressure, while the actual pressure in the monolayer remains lower than the collapse pressure. The nuclei growth from the molecules located inside the excluded surface regions is not possible, given that the promotion of molecules from the monolayer to the domain should be accompanied by a reduction in the enclosed area (approximately a reduction of two-thirds for the trilayer formation). Then, the promotion of molecules from the monolayer to the trilayer is prohibited due to the rigid network of the domains. Initially the domains grow, but the inside area does not decrease in a proportional way. As a consequence, the surface pressure drops inside the enclosed regions. The enclosed regions are transformed into excluded surface regions for the nucleation and growth (see Scheme 1).

SCHEME 1[a]

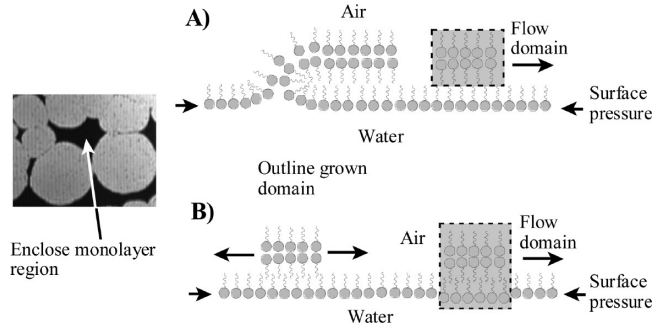

[a] (Left) Zoom of the BAM image corresponding to an enclosed monolayer region (black region). (A) Illustration of a 3D domain consisting of bilayer floating over the monolayer. (B) Illustration of a 3D domain consisting of a trilayer immersed in the monolayer.

Vollhardt and Retter defined the critical surface pressure required for the formation of the 3D nuclei (π_{crit}), and the minimum surface pressure at which the nuclei continue to grow (π_e),[27] being $\pi_e < \pi_{crit}$. The drop of the surface pressure inside the enclosed region must be below π_e.

Excluded surface regions are not expected to be found in monolayers that collapse via folding. In the case of monolayer folding, the surface pressure is applied continuously on the whole monolayer. The drop of the surface pressure in the monolayer would not be possible if the 3D domain consisted of bilayer floating over the monolayer (see Scheme 1A). There is an important conclusion from the previous explanation; in our system the 3D domain must be immersed in the monolayer, in contact with the aqueous subphase, and formed by the trilayer (Scheme 1B). In this way, discontinuity arises, and distinct values of local surface pressure are allowed.

3.5. Absence of Domain Coalescence and/or Deformation: Physical Insights. Under the perspective of the traditional monolayer collapse via trilayer formation, total domain coalescence is assumed to occur. However, as BAM images show, for the DOMA/TSPP mixed monolayer, there is no coalescence and/or deformation of domains, even for an infinite time. This result seems surprising, as it contradicts the classical assumption of total film covering by the trilayer upon collapse. The physical explanation for this phenomenon implies the consideration of an additional parameter, that is, the line tension of the domains. The circular form of the domains indicates the minimization of its perimeter and consequently its energy; therefore the domains must be fluid and should coalesce under surface pressure[28] against what is observed experimentally. Meunier et al.[29,30]

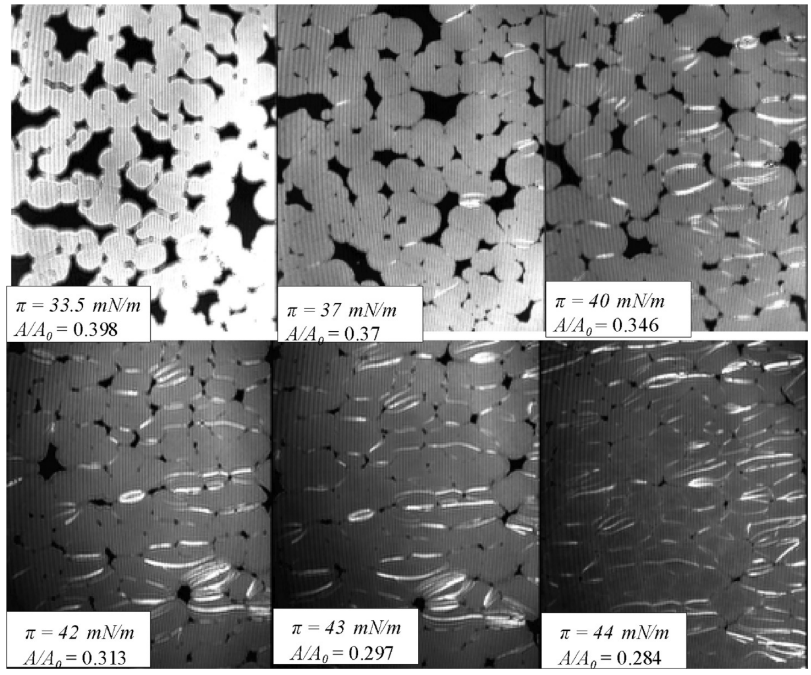

Figure 4. BAM images obtained after a relaxation experiment at $\pi_c = 33.5$ mN/m. After the final step of the collapse process, the surface pressure was increased in steps of 1 mN/m, waiting after each pressure increase to the stabilization of the film. Only BAM images obtained at 37, 40, 42, 43, and 44 mN/m are shown.

suggested that an anisotropic contribution to the line tension is essential to stabilize the domains in determinate situations. Anisotropy in the line tension does not permit the domains to be fused, whereas isotropic line tension allows the domains to be fused while touching each other.[31] The anisotropic line tension could be originated by the different tilt of the lipid at the boundary of the domains, which remember the behavior of the liquid crystal.[32]

Therefore, the monolayer collapse is obviously a change of phase, although this cannot be interpreted exclusively in terms of a thermodynamic equilibrium, intervening, as an additional factor the anisotropic line tension of the domains. A high line tension implies a high resistance to the domain deformation, and the anisotropy of the line tension involves the lack of coalescence between these domains.

In the spirit of obtaining new insights on the line tension influence, a relaxation experiment was performed. In this experiment, a constant surface pressure of $\pi_c = 33.5$ mN/m was applied, allowing the film to reach the final step of the collapse process (see $A/A_0 = 0.398$ in Figure 4). After that, the surface pressure was increased in steps of 1 mN/m, allowing an extra time after each surface pressure increment for the stabilization of the film. Figure 4 shows recorded BAM images obtained from this experiment. As can be seen, with the increasing of surface pressure, A/A_0 decreases lightly, for example, for $\pi = 40$ mN/m, the area decreases to $A/A_0 = 0.346$, but neither the coalescence nor the deformation domain are evident. At $\pi = 40$ mN/m, the appearance of bright streaks at the contact line between domains is observed. The bright streaks may be related with the superposition of neighboring domains. Moreover, the appearance of new nuclei in the black regions of the film cannot be observed.

The application of a surface pressure above 40 mN/m results in domain deformation, but no domain coalescence was observed. For this surface pressure the domains are forced to grow with a noncircular geometry. At 44 mN/m, the excluded surface regions (black monolayers region) disappear almost completely being the fraction of dark area less than 1%. In this experiment the surface pressure π_e is reached inside the excluded surface regions, but the π_{crit} is not reached.

3.6. Revisiting NGC Theory: Accounting for Partial Collapse. For the NGC theory, A_∞ is defined as the area when the interface is completely covered with domains with homogeneous structures. The fulfillment of eq 1 implies that neither the rate of nucleation nor the rate of growth of nuclei change over the whole relaxation process, and that the growing nuclei coalesce as a final stage of the process. This assumption leads to a complete collapse of the monolayer at infinite time: the whole monolayer is converted into a trilayer structure. However, if the collapse is not completed, the experimental area A_∞ represents an apparent value without physical meaning as referring to the model represented by eq 1.

The absence of coalescence between domains prevents us to apply the eq 1, at least for the full relaxation period observed in Figures 1−3. During the first stages of the nucleation, when there is no collision between nuclei, the A_∞ value must correspond to a hypothetical situation where the entire surface should be coated by the domains. Therefore, it is not correct to use the apparent value $A_\infty/A_0 \approx 0.4$, as was used previously for the numerical fit shown in Figure 3 (solid line). This fact was considered previously by Rugonyi et al.,[17] who assumed that for a trilayer transformation A_∞ must be one third of the A_0.

If θ is defined as the surface fraction occupied by the domains, as observed by BAM, then, A/A_0 is expressed as

$$\frac{A}{A_0} = (1 - \theta) + \frac{A_\infty}{A_0}\theta \qquad (2)$$

Thus, when $A/A_0 \approx 0.4$ (final step of monolayer collapse at a constant π_c, Figure 2), the surface fraction recovered by the domains is $\theta \approx 0.8 - 0.85$, therefore from the eq 2, $A_\infty/A_0 \approx 0.25 - 0.29$, i.e. as $A_0 \approx 0.75$ nm^2, then $A_\infty \approx 0.19$ - 0.22 nm^2. This calculated A_∞/A_0 value agrees with the experimental value

obtained at $\pi = 44$ mN/m, from Figure 4 where the total surface is almost covered with trilayer. The experimentally obtained area reduction is slightly lower than that expected for a trilayer formation (from $A_0 \approx 0.75$ nm^2, to $A_\infty \approx 0.25$ nm^2). This difference is ascribed to an arrangement somewhat more compact of the molecules in the domain than in the monolayer.

Fitting the experimental A/A_0 versus t data to eq 1, for $A/A_0 > 0.8$ (implying $\theta < 0.28$) an improved agreement between calculated and experimental data is obtained, as shown in Figure 3B. Using $A_\infty/A_0 = 0.28$, t_{ind}, k, and n can be calculated. Figure 3B shows the experimental data for $\pi_c = 35$ mN/m (gray dotted line), and the predictions of eq 1 (dashed line). The values of the parameters obtained were as follows: $t_{ind} = -12$ s, $k = 7.296 \times 10^{-3}$ s^{-n}, and $n = 2.94$. As can be seen from Figure 3B [ln(A/A_0) vs t], for the region of lower times, there is an excellent agreement between experimental data and theoretical predictions. The value $n \approx 3$ was obtained by using values of A_∞/A_0 ranging between 0.25−0.29. Furthermore, $n \approx 3$ is obtained for all the analyzed π_c values. This n value implies that the rate of the radial growth of a nucleus, considered to be a circular disk, does not vary with time and that the nucleation is progressive (small rate constant).[5]

Therefore, the application of the NGC theory should be realized with caution. Equation 1 is applicable in the full range of time only when the coalescence of the domain takes place.

3.7. The Kinetics of the Return of the Collapsed Material to the Monolayer: Trilayer to Monolayer Transition. The collapse of a DOMA/TSPP mixed monolayer is a reversible process.[14] After the monolayer collapse reaches its final point, the molecular area maintains a constant value. Film structure, as formed by both monolayer and trilayer regions, may be decompressed by using a new constant surface pressure value, π_d. The surface pressure π_d should be slightly below π_c. For a $\pi_d \geq 30$ mN/m, the film area does not increase, indicating that the monolayer recovering from the trilayer does not occur. However, for $\pi_d < 30$ mN/m an expansion of the film was observed. Figure 1 shows the A/A_{Max} versus t expansion curve for $\pi_d = 25$ mN/m (dashed line).

Vollhardt and Retter demonstrated, by using a two-step surface pressure experiment, that at the equilibrium surface pressure π_e the preformed nuclei cease to grow.[27] The decompression experiment described here is also a two-step surface pressure experiment. The difference is that for our case $\pi_d < \pi_e$ and therefore the nuclei must decrease for an ideal case. From a formal perspective, the NGC theory (eq 1) can be applied to a phase-change 3D → 2D. The main consideration is that the monolayer and trilayer exchange their roles. That is, the monolayer is the final state. The initial state is a mixed monolayer and trilayer state. Values of A_0 and A_∞ are also exchanged. The maximum area in this expansion process coincides with the area at the end of the experiment, $A_\infty = A_{max}$.

Figure 5 shows BAM images obtained during the expansion process. As can be seen, the bright domains (trilayer) decrease in size, while retaining their circular form, approximately. Eventually, bright domains disappear completely. In none of the expansion experiments, the occurrence of holes, that is, dark regions due to the monolayer formation, inside the domain was observed.

For the film expansion process, A_0 is the theoretical area for a film completely formed as a trilayer. This A_0 area is not experimentally accessible. In this case A_0 corresponds to the area A_∞ for the compression process. For the monolayer expansion process, A_∞ is the area for the monolayer, as completely recovered, at $\pi = 25$ mN/m. This A_∞ value can be measured experimentally ($A_\infty \approx 0.82$ nm^2, see inset in Figure 1). In this way, eq 1 can be easily transformed for decompression into

$$\frac{A(t)}{A_\infty} = 1 + \frac{(A_0 - A_\infty)}{A_\infty} \exp[-k(t - t_{ind})^n] \qquad (3)$$

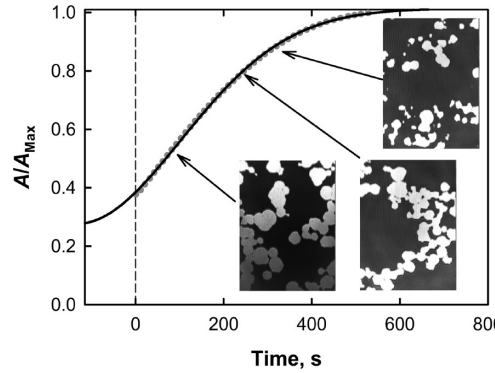

Figure 5. Gray dotted line: experimental A/A_∞ vs t (where $A_\infty = A_{Max}$) for $\pi_d = 25$ mN/m. Solid line: predictions of eq 3 for; $A_0/A_\infty = 0.26$, $t_{ind} = -130.3$ s, $k = 1.19 \times 10^{-5}$ s^{-n}, and $n = 1.95$. Also some BAM images obtained during the expansion process are shown.

The fit of the experimental data (A/A_∞ vs t) to eq 3 by using A_0/A_∞, t_{ind}, k, and n as unknown parameters is shown in Figure 5 as a solid line. The obtained parameters were as follows: $A_0/A_\infty = 0.26$, $t_{ind} = -130.3$ s, $k = 1.19 \times 10^{-5}$ s^{-n}, and $n = 1.95$. It should be noted that in this case, there is coalescence between monolayer regions. Therefore, all the set of experimental data could be used for the numerical fit of eq 3. The possibility of using experimental data recorded during all the expansion time is a fundamental difference with the collapse process, where only the initial data may be used, due to the lack of coalescence between domains.

As $A_\infty \approx 0.82$ nm^2, and $A_0/A_\infty = 0.26$, $A_0 \approx 0.21$ nm^2 is obtained. A_0 corresponds to the theoretical area when the film is completely formed as a trilayer, a value coincident with the previously obtained. The negative value of t_{ind}, accounts for the time required for an interface fully covered by the trilayer to reach the starting point of the expansion experiment ($t = 0$, see Figure 5). The values of $n \approx 2$ were obtained for all the experiments performed. This value is consistent with an instantaneous nucleation with cylindrical edge growth. It is noticeable that for the collapse process the nucleation was progressive, whereas for the inverse process the nucleation was instantaneous.

The conceptual difficulty involved in defining the critical size of the nucleus and the nucleation rate for the inverse process of the collapse is worthy of special note. One may assume that after the 3D film is formed and π_d is applied, some holes (monolayer) are formed. These holes in the 3D phase will be unstable unless they reach a given critical size. The number of such critically sized holes will be the equivalent to the number of nuclei for the condensation, being positive the hole growth rate. With these considerations, eq 3 is acceptable and the collapse reversible.

Despite the formal equivalence between nucleation and its inverse process, theoretical difficulties arise in the case of an interface completely covered by a trilayer or a more compact film. For a case of a trilayer under expansion, the monolayer should be formed from the holes appearing inside the trilayer domain. However, the creation of these holes inside the domain

trilayer is highly improbable, since the area occupied by a molecule in the monolayer is three times larger than the molecular area occupied in the trilayer, approximately. A 3D rigid domain with high line tension cannot be expanded due to hole formation without a fracture of the whole crystalline lattice; the energy cost to cause such a fracture may be very high. The irreversibility of many collapse processes could be caused by this phenomenon. The return from an interface completely covered by collapsed material with high line tension in the monolayer state is only possible at the barrier, at the perimeter of the Langmuir trough, or through the film fractures. For these cases, the collapse will be irreversible.

For our case, the absence of holes inside the domains in the expansion process (see Figure 5) is an indication of the absence of the creation of holes. Therefore, it is assumed that all holes were created instantaneously at the beginning of the expansion process (negative time regions in Figure 5). This fact gives an explanation as to why the nucleation process for the 3D → 2D transition is instantaneous. In fact, the holes (monolayer) already exist since the domains do not coalesce during the collapse (exclude regions). One consequence of the above reasoning is that the collapse is reversible for our system, and therefore the relaxation process follows the model of eq 3, because of the absence of domain coalescence during the collapse. A general conclusion may be drawn from this study: the collapse of condensed phases can be reversible only if the domains do not coalesce previously, at least for domains with high line tension.

4. Conclusions

The reversible collapse of a mixed monolayer DOMA/TSPP in a molar ratio 4:1 has been described thanks to BAM images and theoretical modeling. The collapse mechanism occurs via trilayer formation. Trilayer regions appear as bright domains with circular forms. Along the collapse process, the bright domains increase their size, but they neither coalesce nor are deformed with compression. Moreover, in the final step of the collapse there are regions in which the monolayer persists. These monolayer regions are enclosed by the surrounding trilayer domains and isolated from each other.

The presence of the monolayer in the final step of the collapse has been explained in terms of the drop of the surface pressure inside the enclosed regions. The collision between collapsed domains might form an interconnected rigid network that sustains extra pressure, while the actual pressure in the monolayer remains lower than the collapse pressure. The nuclei growth from the molecules located inside the monolayer enclosed regions are not possible, given that the promotion of molecules from the monolayer to the domain should be accompanied by a reduction in the enclosed area (approximately a reduction of two-thirds for the trilayer formation). Then, the promotion of molecules from the monolayer to the trilayer is prohibited due to the rigidity of the domains. Initially the domains grow, but the inside areas do not decrease in a proportional way. As a consequence, the surface pressure drops inside the enclosed regions. An important conclusion is that the domain must be formed by the trilayer (Scheme 2B) and not by bilayer floating over the monolayer.

In the case of high values of the collapse surface pressures, the domains can grow in a noncircular way, eventually filling the observed surfaces completely. Under this condition of high surface pressure, the domains never coalesce due to their anisotripic line tension. The monolayer collapse process is a phase change. However, the monolayer collapse cannot be interpreted exclusively in terms of thermodynamics equilibrium, intervening as an additional factor, the anisotropic line tension of the domains. A high line tension of a given domain implies a high resistance to deformation, and the anisotropy of the line tension the lack of coalescence between domains. Because of the lack of coalescence, the NGC theory (eq 1) cannot be applied to the DOMA/TSPP collapse at least for the full relaxation time range. For short times and according to the NGC theoretical model, the collapse corresponds to a progressive nucleation with cylindrical edge growth.[5]

The collapse of the DOMA/TSPP system is reversible. Thus, the return kinetics from 3D → 2D phases could be analyzed from the NGC theory. For this expansion process, the monolayer and trilayer exchange roles. It is noticeable that for the collapse process the nucleation was progressive, whereas for the reverse process the nucleation was instantaneous. For a decompressing interface that is completely covered with trilayer at the initial time, or a more compact film, the monolayer should be formed from the holes appearing inside the trilayer film. However, the creation of these holes inside the condensed films is highly improbable, since the area occupied by a molecule in the monolayer is three times greater than that which occupies the trilayer, approximately. A 3D rigid and homogeneous film cannot expand toward the monolayer through the hole formation without a fracture. The irreversibility of many collapse processes could be caused by this phenomenon. The return of the collapsed material toward the monolayer is only possible at the perimeter of the Langmuir trough or through of fractures of the films.

However, for 3D structures formed by domains that do not completely cover the interface, the return to the monolayer takes place at the perimeter of the domains without hole formation inside the domains that is coherent with an instantaneous nucleation process. The reversible character of the collapse is probably due to the lack of coalescence between domains that favor the return of the molecules toward the monolayer.

Acknowledgment. We thank the Spanish CICYT for financial support of this research in the framework of Project CTQ2007-64474/BQU (FEDER A) and also thank the Junta de Andalucía (Consejería de Innovación, Ciencia y Empresa) for special financial support P06-FQM-01698 and P08-FQM-4011. A.M. González-Delgado and J.J. Giner-Casares thank the Ministerio de Ciencia e Innovación for their FPI fellowships.

Supporting Information Available: This material is available free of charge via the Internet at http://pubs.acs.org.

References and Notes

(1) Rapaport, H.; Kuzmenko, I.; Belfeld, M.; Kjaer, K.; Als-Nielsen, J.; Popovitz-Biro, R.; Weissbuch, I.; Lahav, M.; Leiserowitz, L. *J. Phys. Chem. B* **2000**, *104*, 1399.

(2) Lee, K. Y. C. *Annu. Rev. Phys. Chem.* **2008**, *59*, 771.

(3) Gaines, G. L. *Insoluble Monolayers at Liquid-Gas Interface*; Interscience: New York, 1966.

(4) Smith, R. D.; Berg, J. C. *J. Colloid Interface Sci.* **1980**, *74*, 273.

(5) Vollhardt, D.; Retter, U. *J. Phys. Chem.* **1991**, *95*, 3723.

(6) Wagner, J.; Michel, T.; Nitsch, W. *Langmuir* **1996**, *12*, 2807.

(7) Chen, X.; Wiehle, S.; Weygand, M.; Brezesinski, G.; Klenz, U.; Galla, H. J.; Haufe, G.; Chi, L. *J. Phys. Chem. B* **2005**, *109*, 19866.

(8) Vaknin, D.; Bu, W.; Satija, S. K.; Travesset, A. *Langmuir* **2007**, *23*, 1888.

(9) Bu, W.; Vaknin, D. *Langmuir* **2008**, *24*, 441.

(10) Mul, M. N. G. D.; Mann, J. A. *Langmuir* **1994**, *10*, 2311.

(11) Salfer, R.; Michel, T.; Nitsch, W. *Colloid Surf., A:* **2002**, *210*, 253.

(12) Gourier, C.; Knobler, C. M.; Daillant, J.; Chatenay, D. *Langmuir* **2002**, *18*, 9434.

(13) Schief, W. R.; Antia, M.; Discher, B. M.; Hall, S. B.; Vogel, V. *Biophys. J.* **2003**, *84*, 3792.

(14) Perez-Morales, M.; Pedrosa, J. M.; Martin-Romero, M. T.; Möbius, D.; Camacho, L. *J. Phys. Chem. B* **2004**, *108*, 4457.

(15) Deng, J. J.; Viers, B. D.; Esker, A. R.; Anseth, J. W.; Fuller, G. G. *Langmuir* **2005**, *21*, 2375.
(16) Kundu, S.; Datta, S.; Hazra, S. *Langmuir* **2005**, *21*, 5894.
(17) Rugonyi, S.; Smith, E. C.; Hall, S. B. *Langmuir* **2005**, *21*, 7303.
(18) Kundu, S.; Datta, A.; Hazra, S. *Langmuir* **2008**, *24*, 9386.
(19) Nikomarov, E. S. *Langmuir* **1990**, *6*, 410.
(20) Siegel, S.; Honig, D.; Vollhardt, D.; Mobius, D. *J. Phys. Chem.* **1992**, *96*, 8157.
(21) Vollhardt, D. *Adv. Colloid Interface Sci.* **1993**, *47*, 1.
(22) Vollhardt, D.; Ziller, M.; Retter, U. *Langmuir* **1993**, *9*, 3208.
(23) Vollhardt, D. *Adv. Colloid Interface Sci.* **2006**, *123*, 173.
(24) Avrami, M. *J. Chem. Phys.* **1939**, *7*, 1103.
(25) Avrami, M. *J. Chem. Phys.* **1940**, *8*, 212.
(26) Avrami, M. *J. Chem. Phys.* **1941**, *9*, 177.
(27) Vollhardt, D.; Retter, U. *Langmuir* **1998**, *14*, 7250.
(28) Vollhardt, D. *Colloid Surf. A: Physicochem. Eng. Aspects* **1998**, *143*, 185.
(29) Hénon, S.; Meunier, J. *J. Chem. Phys.* **1993**, *98*, 9148.
(30) Riviére, S.; Meunier, J. *Phys. Rev. Lett.* **1995**, *74*, 2495.
(31) Mufazzal-Hossain, M.; Kato, T. *Langmuir* **2000**, *16*, 10175.
(32) Yamamoto, T.; Manaka, T.; Iwamoto, M. *Eur. Phys. J. E* **2009**, *29*, 1.

JP9055158